HETEROCYCLES, Vol. 104, No. 11, 2022, pp. 1935 - 1953. © 2022 The Japan Institute of Heterocyclic Chemistry
Received, 29th June, 2022, Accepted, 20th September, 2022, Published online, 27th September, 2022
DOI: 10.3987/COM-22-14708

SYNTHESIS AND UTILIZATION OF TETRAHYDRONAPHTHALENE-1,3-DICARBONITRILE AS A SOURCE OF BENZO[*f*]QUINAZOLINE, PYRIDINE, IMIDAZOLE DERIVATIVES WITH ANTITUMOR ACTIVITY AND MOLECULAR DOCKING AND DYNAMICS STUDIES

Marwa El-Hussieny,[1] Fatma A. A. El-Hag,[2] Ahmed A. El-Rashedy,[2] and Ewies F. Ewies[1]*

[1]Organometallic and Organometalloid Chemistry Department, National Research Centre, 33 ElBohouth St., (Former El Tahrir) Dokki, P.O. 12622, Giza, Egypt.
[2] Chemistry of Natural and Microbial Products Department, National Research Centre, 33ElBohouth St., (Former El Tahrir) Dokki, P.O. 12622, Giza, Egypt.

Abstract – Seventeen new compounds of benzo[*f*]quinazoline, pyridine, and imidazole derivatives were prepared *via* reaction of 2-amino-4-phenyl-5,6,7,8-tetrahydronaphthalene-1,3-dicarbonitrile (**1**) with carbon disulfide, urea, thiourea, formic acid, formamide, acetonitrile, acetic anhydride, phenyl isocyanate, phenyl isothiocyante, and triethyl orthofromate followed by cyclization with hydrazine hydrate to give pyrimidine derivatives **2-10**. Besides that, reaction of compound **1** with 2-benzylidenemalononitrile or with ethyl acetoacetate afforded pyridine derivatives **11** and **12**. Also, compound **1** reacted with ethylenediamine or *o*-phenylenediamine to give imidazole derivatives **13a-d**. Structures of the isolated new products were elucidated by compatible analytical and spectroscopic measurements. Moreover, antitumor activity of all new compounds is studied. Compound **3b** is the most active compound among these derivatives against two cancer cell lines (MCF7, HepG2) in comparison with Doxorubicin as a reference drug. Computational modeling of studied DNA-ligands systems reveals that **3b** compound can potentially inhibit DNA dodecamerd target thereby creating a pathway toward DNA targeting approach in the anticancer treatment.

INTRODUCTION

Tetrahydronaphthalene (tetralin) is an important hydrocarbon system which is present in various biologically active drugs such as Idarubicin, Daunorubicin (anti-leukemic drugs), Doxorubicin (anticancer

drug), and Epirubicin (treat breast cancer) (Figure 1). Also, benzo[*f*]quinazoline is a two fused six membered ring with pyrimidine reported in literature for its biological activity. It is used medicinally as antimalarial agents and it presents in many drugs[1] such as Prazosin (for treatment of high blood pressure), Gefitinib (for treatment of certain types of cancer), Erlotinib (for treatment of lung and pancreatic cancers), Trimetrexate (antineoplastic and antiparasitic agents), and Anagrelide (for treatment of thrombocytosis) (Figure 1).

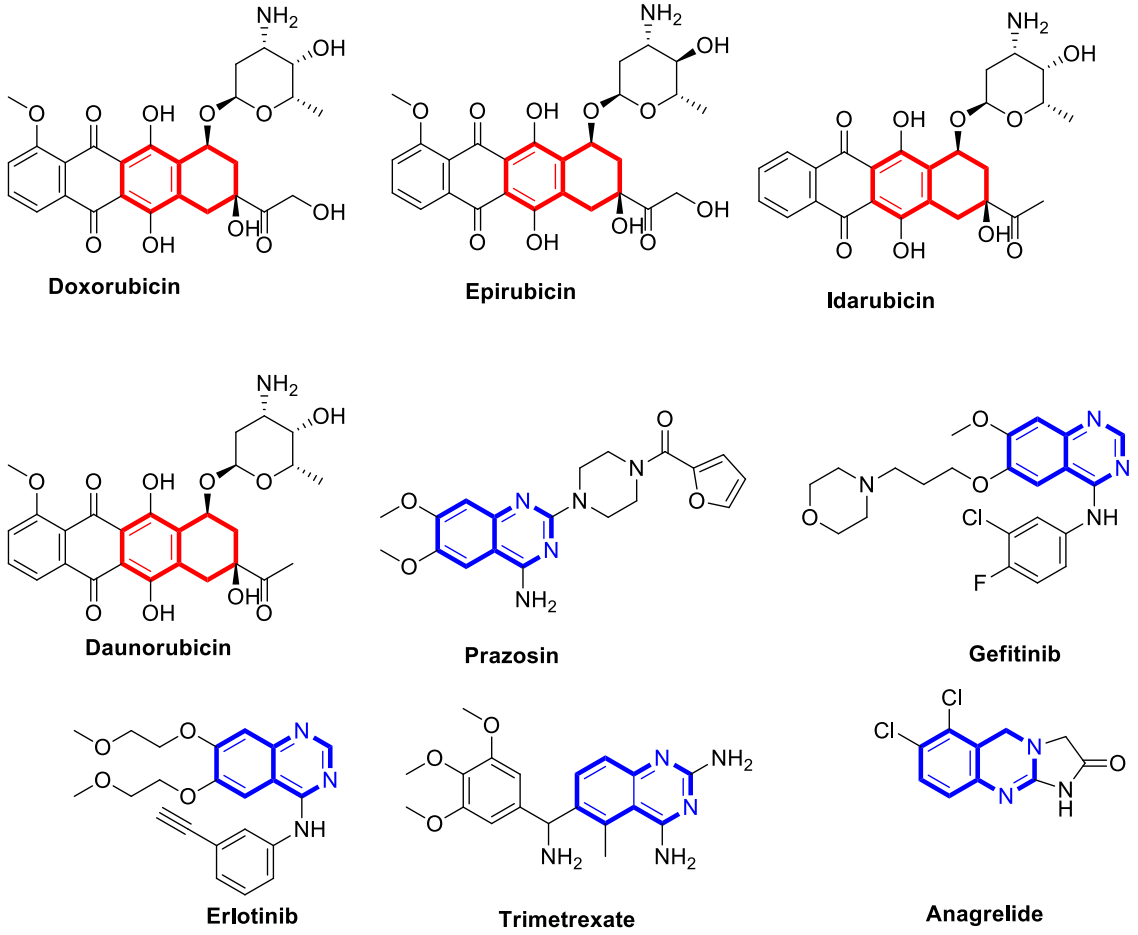

Figure 1. Biologically active drugs that have tetralin and benzo[*f*]quinazoline moieties

Besides that, o*rtho*-aminonitrile derivatives are attractive key intermediates[2] for the synthesis of many heterocyclic molecules,[3] such as quinolines,[4] isoquinolines,[5] benzodiazipines,[6] benzo[*f*]quinazoline,[1,7] and many related compounds having pyrimidine moiety as a part of their structures described as potentially active compounds as anticancer,[8] antimicrobial,[9] antiviral,[10] antifungal[11] and anti-inflammatory[12] activities. Also, it has been reported that the efficient designed drugs with highly biological activity can be synthesized *via* incorporation of two or more heterocyclic derivatives. Based on the above survey and in continuation of our interest in this topic,[13] we report herein one-pot method for rapid synthesis and high yield of compound **1** according to the literature (Scheme 1),[14] and utilizing as a source of various carbocyclic and

heterocyclic analogues of benzo[*f*]quinazoline, pyridine and imidazole derivatives to study their activity as antitumor agents against two cell lines (MCF-7, HepG2) according to MTT assay.

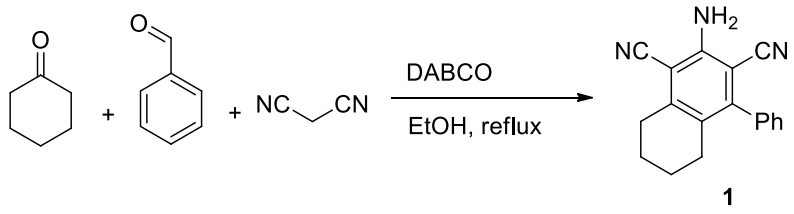

Scheme 1. Synthesis of starting material

RESULTS AND DISCUSSION

Seventeen new compounds were prepared, their structures were determined according to spectroscopic and analytical analyses and this is outlined in the following Schemes 1-3 and Figure 2. When compound **1** smoothly reacted with excess carbon disulfide in pyridine at reflux temperature, 6-phenyl-1,3-dithioxo-1,2,3,4,7,8,9,10-octahydrobenzo[*f*]quinazoline-5-carbonitrile (**2**) was precipitated as yellow color crystals in a 75% yield (Scheme 2). Compatible analytical and spectroscopic results were appeared in good with the assigned structure **2** (*cf*. Experimental). Thus, microanalyses and molecular weight determination (MS) for **2** corresponded to $C_{19}H_{15}N_3S_2$ (MS (*m/z*): M^+ 349, 15%). Infrared (IR) of **2** revealed strong absorption bands at 3175 (NH), 1335, 1330 (C=S), 2220 (CN) cm^{-1}. Also, the ^1H NMR spectrum of **2** (DMSO-d_6, δ, ppm) showed protons as two singlets at 9.78 and 9.08 (2 NH), two triplets at 3.39, 3.04 (2 CH_2), and two multiples at 2.12, 1.98 (2 CH_2) of cyclohexane.

Also, compound **1** reacted with urea or thiourea *via* fusion at oil bath, it affects cyclization to give the corresponding derivatives **3a**,**b** in a good yield which were proved by analytical and spectral analyses (Scheme 2).

1-Oxo-6-phenyl-1,2,7,8,9,10-hexahydrobenzo[*f*]quinazoline-5-carbonitrile (**4**) was obtained *via* the reaction of **1** with formic acid at reflux temperature, while 1-amino-6-phenyl-7,8,9,10-tetrahydrobenzo[*f*]quinazoline-5-carbonitrile (**5**) was obtained *via* reaction of **1** with formamide in DMF at reflux temperature (Scheme 2). The structures of compounds **4** and **5** were elucidated according to compatible spectroscopic analyses (*cf*. Experimental).

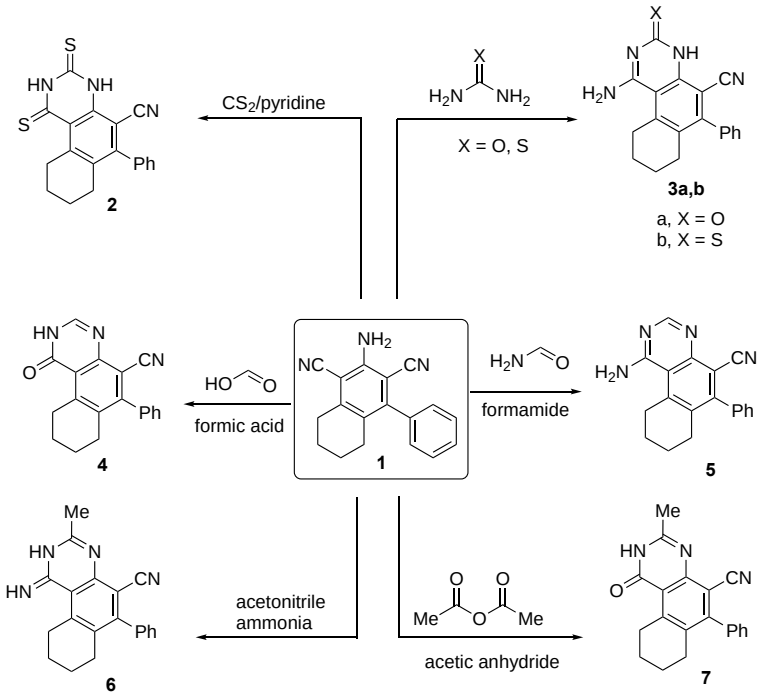

Scheme 2. Synthesis of compounds **2-7**

Further, 1-amino-; and 1-oxo-3-methyl-6-phenyl-1,2,7,8,9,10-hexahydrobenzo[*f*]quinazoline-5-carbonitrile (**6**,**7**) were obtained when compound **1** was allowed to react with acetonitrile in the presence of ammonia and with acetic anhydride at reflux temperature, respectively (Scheme 2).

Also, to furnish more pyrimidine derivatives, phenyl isocyanate or phenyl isothiocyanate was reacted with compound **1** at reflux temperature to give 1-imino-3-oxo- (or 3-thioxo)-2,6-diphenyl-1,2,3,4,7,8,9,10-octahydrobenzo[*f*]quinazoline-5-carbonitrile (**8a**,**b**) in high yield (Scheme 3). Also, triethyl orthoformate was allowed to reacted with compound **1** in EtOH at reflux temperature in the presence of sodium ethoxide to afford ethyl *N*-(1,3-dicyano-4-phenyl-5,6,7,8-tetrahydronaphthalen-2-yl)formimidate (**9**) which cyclized to iminopyrimidine derivative **10** when reacted with hydrazine hydrate in *n*-butanol (Scheme 3).

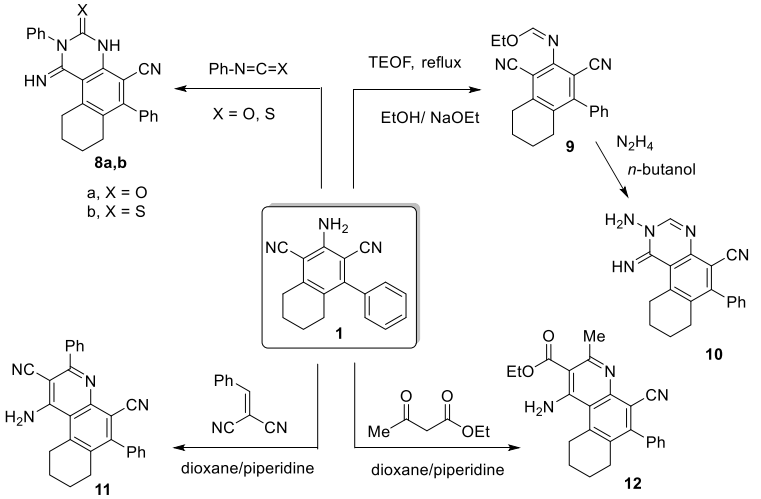

Scheme 3. Synthesis of compounds **8-12**

Malononitrile was condensed with benzaldehyde to furnish 2-benzylidenemalononitrile which reacted with compound **1** in basic medium and dioxane to give the pyridine derivatives **11**, while under the same conditions, ethyl 1-amino-5-cyano-3-methyl-6-phenyl-7,8,9,10-tetrahydrobenzo[*f*]quinoline-2-carboxylate (**12**) was obtained through reaction of **1** with ethyl acetoacetate (Scheme 3). Structures of compounds **8a**,**b**-**12** were confirmed on the basis of analytical and spectroscopic analyses (*cf.* Experimental).

Finally, the corresponding imidazole derivatives **13a**,**b** were obtained via reactions of starting material **1** with ethylenediamine or *o*-phenylenediamine in the presence of CS_2 as solvent, while these reactions were proceeded with two moles of ethylenediamine or *o*-phenylenediamine under the same conditions to afford the bis-imidazole derivatives **13c**,**d** respectively (Figure 2). Spectroscopic and analytical analyses elucidated the structures of compounds **13a-d** (*cf.* Experimental).

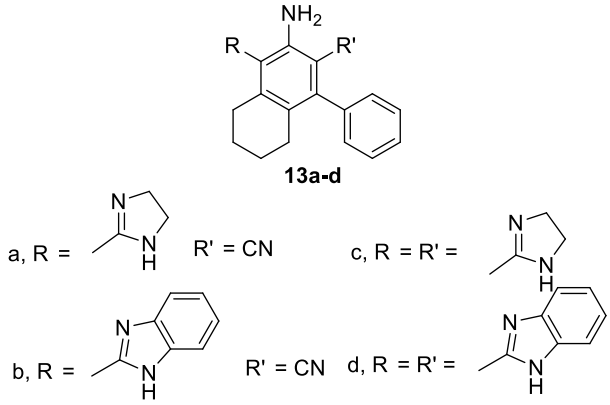

Figure 2. Synthesis of compounds **13a-d**

BIOLOGICAL ACTIVITY

IN VITRO ANTICANCER ACTIVITY

IN VITRO ANTI-PROLIFERATIVE ACTIVITY AND SELECTIVITY

Cancer is a group of more than one hundred diseases involving abnormal cell growth and there are many attempts to prepare new heterocyclic compounds with more efficiency and low cost than drugs that are used in treatment of cancer, so, as mentioned in this work, benzo[*f*]quinazoline derivatives have received considerable attention owing to their activity in many anticancer drugs. Thus, this study was tailored to screen *in vitro* activity of these new compounds against two cancer cell lines (MCF7, HepG2) according to the MTT assay.

According to Table 1, for breast cancer cell lines (MCF7), compounds **3b**, **5**, **6**, **8b**, **11** revealed high half inhibitory concertation (IC_{50}) in comparison with Doxorubicin as a reference drug (IC_{50} = 26.9±3.9 µM). 1-Amino-6-phenyl-3-thioxo-3,4,7,8,9,10-hexahydrobenzo[*f*]quinazoline-5-carbonitrile (**3b**) is the most active compound in between these derivatives with IC_{50} = 28.7 ± 5.1 µM. The descending order of anticancer activity of all compounds against MCF7 cell lines is **3b**, **11**, **6**, **5**, **8b**, **8a**, **3a**, **13d**, **12**, **10**, **13a**, **7**, **13b**, **13c**,

2, **9**, **1**.

For liver cancer cell lines (HepG2), compounds **3a**,**b** showed anticancer activity which is closed to activity of Doxorubicin with IC_{50} = 12.9 ± 2.2 and 12.6 ± 2.1 µM, then compound **6** with IC_{50} 13.8± 2.5 µM. The descending order of anticancer activity of all compounds against HepG2cell lines is **3b**, **3a**, **6**, **8b**, **10**, **2**, **9**, **12**, **11**, **13c**, **8a**, **13a**, **13b**, **13d**, **7**, **4**, **1**, **5**.

Table 1. IC_{50} of the synthesized compounds against the two cancer cell lines (MCF7, HepG2) according to the MTT assay

Compound Code	IC_{50} (µM) ± SD	
	MCF7	HepG2
1	68.1 ± 5.6	30.5 ± 3.8
2	45.3 ± 5.9	17.5 ± 4.1
3a	36.8 ± 4.7	12.9 ± 2.2
3b	28.7 ± 5.1	12.6 ± 2.1
4	43.4 ± 4.9	29.0 ± 5.1
5	31.3 ± 5.2	49.9 ± 6.5
6	31.0 ± 3.9	13.8 ± 2.5
7	42.4 ± 4.5	26.3 ± 4.9
8a	36.3 ± 3.9	24.8 ± 4.3
8b	32.8 ± 5.5	15.1 ± 2.9
9	49.6 ± 5.8	19.5 ± 2.9
10	41.9 ± 5.6	17.2 ± 2.4
11	30.6 ± 4.9	22.3 ± 4.2
12	36.9 ± 5.1	20.5 ± 2.7
13a	42.8 ± 5.5	23.8 ± 2.5
13b	45.6 ± 5.8	24.3 ± 4.9
13c	49.9 ± 5.6	22.8 ± 4.3
13d	35.6 ± 4.9	25.1 ± 2.9
Doxorubicin	26.9 ± 3.9	10.4 ± 2.6

MOLECULAR DOCKING AND DYNAMICS STUDIES

Based on the *in vitro* anticancer assays, the most active compounds **3b and 6** were selected for further computational studies to investigate their mechanism of action at the molecular level. The binding affinity

and interaction of compounds **3b** and **6** with DNA were predicted using molecular docking simulation studies. Based on the Pharm Mapper Server screening,[15] a preliminary molecular docking simulation was performed to assess the putative binding mode of compounds **3b** and **6** with the proposed targets. Then molecular dynamic simulations were conducted to investigate these potential inhibitors' inhibitory mechanism and selectivity impact toward this target DNA receptor.

Computational modeling of the studied DNA-ligands systems reveals that lead compounds **3b** and **6** can potentially interact with the minor groove of DNA duplex sequence, thereby creating a pathway toward interfering with the activity of DNA processing enzyme by interfering with the transcription factors binding to their respective DNA recognition sequence.[16]

MOLECULAR DYNAMICS (MD) AND SYSTEM STABILITY

To study the inhibitory effectiveness and interactions of putative ligands with DNA targets, MD simulations were carried out. The validation of system stability is essential to trace disrupted motions and avoid artifacts that may develop during the simulation. In this study, Root-Mean-Square Deviation (RMSD) was assessed to measure the systems' stability during the 50 ns simulations. The recorded average RMSD values for all frames of systems **3b**-DNA and **6**-DNA were 2.22 Å, and 2.27 Å, respectively (Figures 3 **A**). These results revealed that the **3b** complex system acquired a relatively more stable conformation than the other studied system.

During MD simulation, assessing protein structural flexibility upon ligand binding is critical for examining residue behavior and their connection with the ligand.[17] DNA dodecamer nucleotide fluctuations were evaluated using Root-Mean-Square Fluctuation (RMSF) algorithm to evaluate the effect of inhibitor binding towards the respective targets over 50 ns simulations. The computed average RMSF values were 4.33 Å and 4.89 Å for **3b**-DNA and **6**-DNA, respectively. Overall nucleotide fluctuations of individual systems are represented in Figures 3**B**. These values revealed that **3b** has the lower nucleotide fluctuation compared to **6** system inhibition.

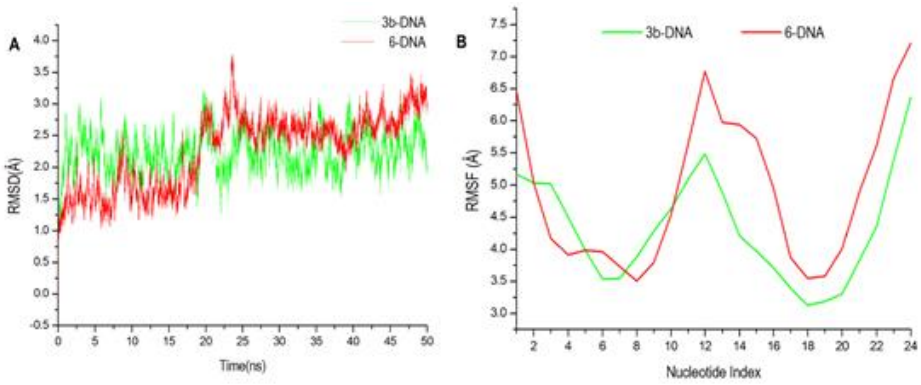

Figure 3. [A] RMSD of ligand interactions **3b**-DNA and **6**-DNA. [B] RMSF of each nucleotide of the DNA

BINDING INTERACTION MECHANISM BASED ON BINDING FREE ENERGY CALCULATION

The structural basis for a ligand's activity is its binding to a specific pharmacological target. As a result, using free binding energy calculations to predict DNA-ligand binding affinities is a promising method for finding novel protein inhibitors.[18] The MM-GBSA program in AMBER18 was used to calculate the binding free energies by extracting snapshots from the trajectories of the systems. As shown in Table 2, all the reported calculated energy components (except ΔG_{solv}) gave high negative values indicating favorable interactions.

Binding free energy (ΔG_{bind}) values -35.69 and -29.74 kcal/mol were obtained for the interactions of DNA nucleotides with compounds **3b** and **6**, respectively. This indicates a more favorable binding of compound **3b** towards DNA than **6**. It is interesting to see how the calculated binding free energy correlated to the experimentally determined IC_{50} values in a good manner.

Table 2. The calculated energy binding for **3b** and **6** against the DNA receptor

Energy Components (kcal/mol)					
Complex	**ΔE_{vdW}**	**ΔE_{elec}**	**ΔG_{gas}**	**ΔG_{solv}**	**ΔG_{bind}**
3b	-36.52± 0.09	-593.12±0.34	-629.65± 0.34	593.95±0.36	-35.69± 0.06
6	-34.58± 0.21	-587.14±0.79	-621.73± 0.86	591.80±0.68	-29.74± 0.30

ΔE_{vdW} = van der Waals energy; Δ_{Eele} = electrostatic energy; ΔG_{solv} = solvation free energy; ΔG_{bind} = calculated total binding free energy.

A close inspection at the individual contribution of energy reveals that the more positive electrostatic energy components drive both **3b** and **6** interactions with the DNA nucleotides, resulting in the reported binding free energies. Substantial binding free energy values were observed in the gas phase for all the inhibition process with values up to -629.65 and -621.73 kcal/mol, respectively. (Table 2).

IDENTIFICATION OF THE CRITICAL NUCLEOTIDES RESPONSIBLE FOR LIGAND BINDING

Figure 4 illustrates the interaction of compound **3b** with minor groove of DNA by forming mainly hydrogen bonds from the amino group of quinazoline with the thymine (DT8, DT10). Further, the benzene ring of quinazoline of **3b** allows it to form hydrophobic interaction with thymine (DT 20). It is worthy to note that a highly electrostatic sulfur atom was found at the base of the hydrophobic pocket of DNA.

In contrast, the quinazoline moiety of ligand **6** had established a hydrogen bond interaction with the thymine

(DT 8, DT9, and DT18).

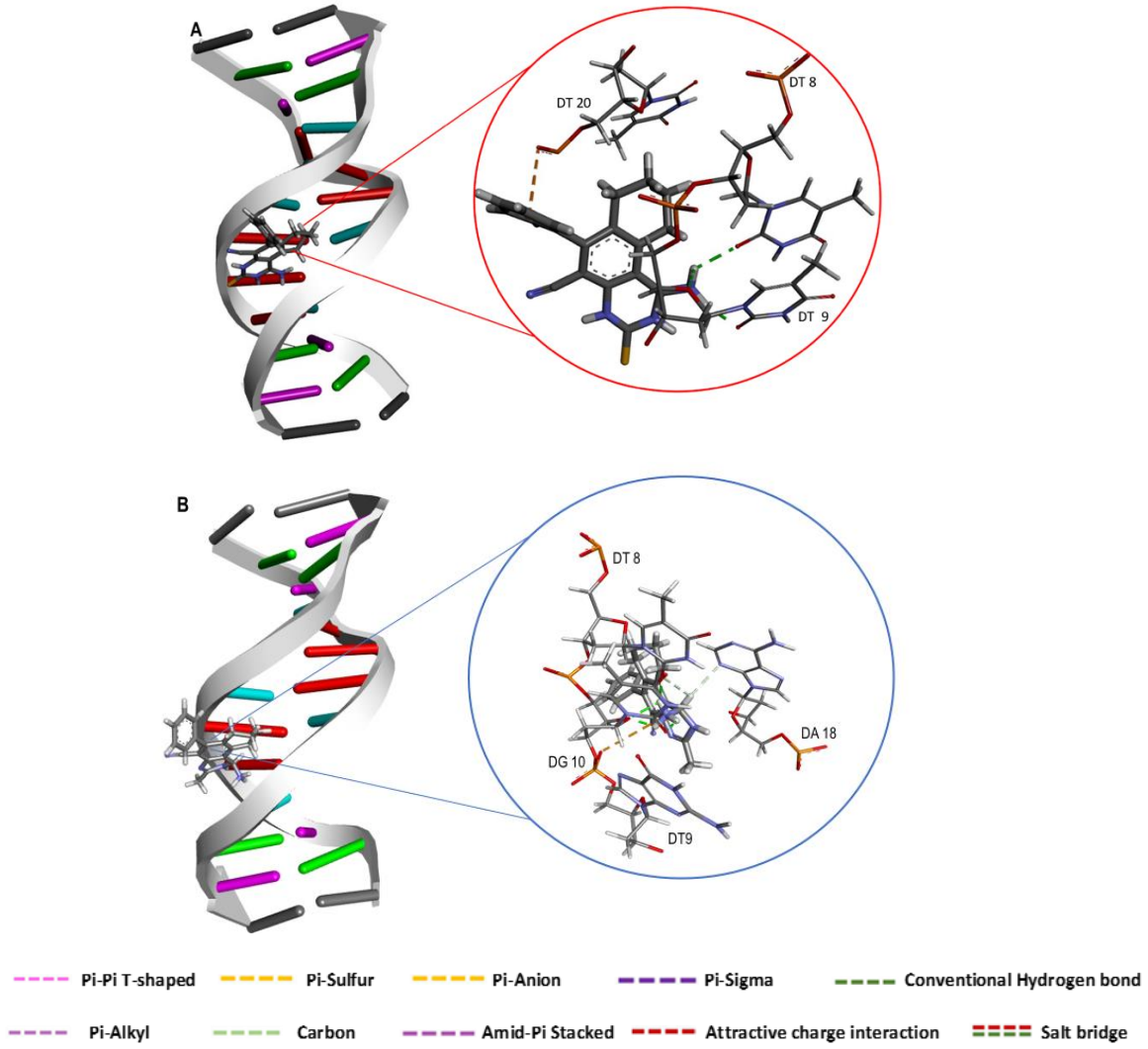

Figure 4. Molecular visualization of interaction between **3b** with DNA (A), and between **6** and DNA (B)

CONCLUSION

From above results, it can be concluded that seventeen new compounds were prepared from tetrahydronaphthalene-1,3-dicarbonitrile as a source of benzo[*f*]quinazoline, pyridine, imidazole derivatives. These compounds were prepared, identified and computational modeling of the studied DNA-ligands systems reveals that **3b** compound can potentially inhibit DNA dodecamerd target thereby creating a pathway toward DNA targeting approach in the anticancer treatment.

EXPERIMENTAL

Melting point of compounds were measured and uncorrected by digital apparatus of Electrothermal IA 9000 series (Electro-thermal, Essex, UK). (See supplementary file)

Synthesis of 2-amino-4-phenyl-5,6,7,8-tetrahydronaphthalene-1,3-dicarbonitrile (1). A mixture of cyclohexanone (0.001 mol), malononitrile (0.002 mol), benzaldehyde (0.01 mol), and DABCO (25 mol%)

in absolute EtOH (15 mL) was refluxed for 5 h. The reaction was monitored with TLC, then evaporated, poured onto ice, extracted with EtOAc, dried over anhydrous Na_2SO_4, filtered, evaporated and then the obtained product was recrystallized from EtOH. Compound **1** was proved by comparing its melting point and Infra-Red spectrum with a reference sample.[14b]

6-Phenyl-1,3-dithioxo-1,2,3,4,7,8,9,10-octahydrobenzo[*f*]quinazoline-5-carbonitrile (2): A compound **1** (1 mmol) in absolute pyridine (15 mL) with excess carbon disulfide were refluxed carefully in water bath for 15 h. During refluxed reaction, a fresh CS_2 was poured twice to reaction mixture. After completion (TLC), it was cooled, poured over acidified crushed ice with hydrochloric acid to afford a precipitate that filtrated, washed with water, dried, and recrystallized from EtOH to afford **2** as yellow crystals in 75% yield: mp 259-260 ºC. IR (KBr, cm^{-1}): 3175 (NH), 3049 (CH-Ar), 2975 (CH aliph), 2220 (CN), 1335, 1330 (C=S). ^{1}H NMR (400 MHz, DMSO-d_6) δ 9.78, 9.08 (2s, 2H, 2 NH), 7.61-7.35 (m, 5H, CH_{arom}), 3.39, 3.04 (2t, 4H, 2 CH_2), 2.12, 1.98 (2 m, 4H, 2 CH_2). ^{13}C NMR (100 MHz, DMSO-d_6) δ 187.9 (C=S), 180.8 (C=S), 143.8, 140.1, 139.4, 138.5, 131.7, 128.6, 128.3, 128.1, 117.2 (aromatic, C-H), 115.7 (CN), 95.9 (***C***-CN), 29.3, 28.7, 23.4 (CH_2). MS (*m/z*): M^+ 349 (15%). Anal. Calcd for $C_{19}H_{15}N_3S_2$ (349.07): % C, 65.30; H, 4.33; N, 12.02; S, 18.35. Found: % C, 65.35; H, 4.30; N, 12.06.

Reaction of 1 with urea and thiourea

General Procedure. Fusion in oil bath is occurred between an equimolar amounts of **1** (0.01 mole) and urea or thiourea (0.01 mole) at 180 ºC for 2-3 h. The reaction mixture was cooled, diluted with EtOH to afford a precipitate, which is filtered off to give compound **3a** or **3b**.

1-Amino-3-oxo-6-phenyl-3,4,7,8,9,10-hexahydrobenzo[*f*]quinazoline-5-carbonitrile (3a) as Yellow crystals in 55% yield: mp 250-252 ºC (EtOH). IR (KBr, cm^{-1}): 3250 (NH_2), 3170 (NH), 3050 (CH-Ar), 2980 (CH aliph), 2221 (CN), 1650 (C=O). ^{1}H NMR (400 MHz, DMSO-d_6) δ 9.08 (s, 1H, 1 NH), 7.59-7.38 (m, 5H, CH_{arom}), 3.03, 2.81 (2t, 4H, 2 CH_2), 1.88, 1.79 (2 m, 4H, 2 CH_2), 1.02 (s, 2H, NH_2). ^{13}C NMR (100 MHz, DMSO-d_6) δ 170.9 (C-NH_2), 153.8 (C=O), 147.8, 143.1, 142.0, 138.4, 131.5, 128.9, 128.5, 128.4, 128.2, 107.2 (aromatic, C-H), 115.5 (CN), 95.5 (***C***-CN), 29.9, 28.5, 23.5, 23.2 (CH_2). MS (*m/z*): M^+ 316 (10%). Anal. Calcd for $C_{19}H_{16}N_4O$ (316.13): % C C, 72.13; H, 5.10; N, 17.71. Found: % C, 72.10; H, 5.15; N, 17.75.

1-Amino-6-phenyl-3-thioxo-3,4,7,8,9,10-hexahydrobenzo[*f*]quinazoline-5-carbonitrile (3b) as Yellow crystals in 65% yield: mp 119-121 ºC (EtOH). IR (KBr, cm^{-1}): 3249 (NH_2), 3180 (NH), 3049 (CH-Ar), 2985 (CH aliph), 2219 (CN), 1350 (C=S). ^{1}H NMR (400 MHz, DMSO-d_6) δ 8.88 (s, 1H, 1 NH), 7.60-7.37 (m, 5H, CH_{arom}), 3.11, 2.80 (2t, 4H, 2 CH_2), 1.80, 1.70 (2 m, 4H, 2 CH_2), 1.06 (s, 2H, NH_2). ^{13}C NMR (100 MHz, DMSO-d_6) δ 183.8 (C=S), 175.9 (C-NH_2), 145.8, 142.5, 142.0, 138.1, 131.0, 128.6, 128.4, 128.2, 107.4 (aromatic, C-H), 115.0 (CN), 94.7 (***C***-CN), 29.6, 29.2, 28.1, 23.1 (CH_2). MS (*m/z*): M^+ 332 (25%). Anal. Calcd for $C_{19}H_{16}N_4S$ (332.11): % C, 68.65; H, 4.85; N, 16.85; S, 9.65. Found: % C, 68.60; H, 4.83;

N, 16.88.

1-Oxo-6-phenyl-1,2,7,8,9,10-hexahydrobenzo[*f*]quinazoline-5-carbonitrile (4): A mixture of compound **1** (0.002 mol) and formic acid (10 mL) was refluxed for 3 h. After completion (TLC), reaction was cooled, poured into ice-water (40 mL) to afford a precipitate which recrystallized from EtOH after filtration to furnish **4**. Pale yellow crystals in 90% yield: mp 161-163 ºC (EtOH). IR (KBr, cm^{-1}): 3190 (NH), 3050 (CH-Ar), 2980 (CH aliph), 2215 (CN), 1640 (C=O). ^{1}H NMR (400 MHz, DMSO-d_6) δ 8.11 (s, 1H, pyrimidine CH), 7.91 (s, 1H, NH), 7.57-7.35 (m, 5H, CH_{arom}), 3.38, 2.74 (2t, 4H, 2 CH_2), 1.77, 1.72 (2 m, 4H, 2 CH_2). ^{13}C NMR (100 MHz, DMSO-d_6) δ 164.8 (C=O), 148.8, 146.5, 145.0, 144.1, 140.0, 138.2, 128.8, 128.7, 128.4, 117.2 (aromatic, C-H), 115.9 (CN), 102.6 (***C***-CN), 29.5, 28.2, 23.6, 23.2 (CH_2). MS (*m/z*): M^+ 301 (35%). Anal. Calcd for $C_{19}H_{15}N_3O$ (301.12): % C, 75.73; H, 5.02; N, 13.94. Found: % C, 75.70; H, 5.06; N, 13.90.

1-Amino-6-phenyl-7,8,9,10-tetrahydrobenzo[*f*]quinazoline-5-carbonitrile (5): Compound **1** (10 mmol) with formamide (10 mL) was heated to reflux in DMF (50 mL) for 15 h (TLC). Reaction mixture was poured into water (100 mL) after cooling to room temperature, and add ammonia solution for neutralization to afford a precipitate which was collected by filtration and washed with water-EtOH, dried and crystallized to give **5**. Pale yellow crystals in 69% yield: mp 165-167 ºC (EtOH). IR (KBr, cm^{-1}): 3290 (NH_2), 3050 (CH-Ar), 2978 (CH aliph), 2210 (CN). ^{1}H NMR (400 MHz, DMSO-d_6) δ 8.28 (s, 1H, pyrimidine CH), 7.55-7.33 (m, 5H, CH_{arom}), 2.88, 2.72 (2t, 4H, 2 CH_2), 1.75, 1.71 (2 m, 4H, 2 CH_2), 0.98 (s, 1H, NH_2). ^{13}C NMR (100 MHz, DMSO-d_6) δ 164.2 (C-NH_2), 158.8 (CH pyrimidine), 152.3, 150.1, 144.5, 138.5, 135.4, 128.5, 128.4, 128.2, 128.0, 122.1, 112.1 (aromatic, C-H), 114.9 (CN) 29.5, 29.2, 28.1, 23.3, 22.2 (CH_2). MS (*m/z*): M^+ 300 (15%). Anal. Calcd for $C_{19}H_{16}N_4$ (300.14): % C, 75.98; H, 5.37; N, 18.65. Found: % C, 75.95; H, 5.40; N, 18.68.

1-Amino-3-methyl-6-phenyl-1,2,7,8,9,10-hexahydrobenzo[*f*]quinazoline-5-carbonitrile (6): Compound **1** (0.002 mol) in MeCN (10 mL) with ammonia was refluxed for 10 h. The reaction was poured into ice-water (40 mL) after cooling to afford a precipitate that recrystallized from EtOH to furnish **6**. Pale yellow crystals in 82% yield: mp 210-212 ºC (EtOH). IR (KBr, cm^{-1}): 3295 (NH_2), 3185 (NH), 3049 (CH-Ar), 2980 (CH aliph), 2211 (CN). ^{1}H NMR (400 MHz, DMSO-d_6) δ 7.62-7.35 (m, 5H, CH_{arom}), 5.02 (s, 1H, cyclic C*H*-NH_2), 2.85, 2.66 (2t, 4H, 2 CH_2), 2.34 (s, 3H, CH_3), 1.72, 1.70 (2 m, 4H, 2 CH_2), 1.61 (s, 2H, NH_2), 1.36 (s, 1H, NH). ^{13}C NMR (100 MHz, DMSO-d_6) δ 157.2 (*C*-CH_2), 146.3, 145.1, 143.5, 138.2, 128.8, 128.5, 128.4, 128.1, 117.2 (aromatic, C-H), 115.9 (CN), 106.1 (*C*-CN), 60.3 (CH-NH_2), 29.3, 28.5, 28.2, 25.2 (CH_2), 20.4 (CH_3). MS (*m/z*): M^+ 316 (25%). Anal. Calcd for $C_{20}H_{20}N_4$ (316.17): % C, 75.92; H, 6.37; N, 17.71. Found: % C, 75.95; H, 6.33; N, 17.67.

3-Methyl-1-oxo-6-phenyl-1,2,7,8,9,10-hexahydrobenzo[*f*]quinazoline-5-carbonitrile (7): Acetic anhydride (10 mL) was added to compound **1** (0.002 mol) under reflux for 3 h (TLC). Evaporation after

cooling, then poured onto ice to afford a precipitate that recrystallized from EtOH to furnish **7**. Yellow crystals in 80% yield: mp 136-138 ºC (EtOH). IR (KBr, cm^{-1}): 3200 (NH), 3051 (CH-Ar), 2981 (CH aliph), 2220 (CN). ^{1}H NMR (400 MHz, DMSO-d_6) δ 7.58-7.32 (m, 5H, CH_{arom}), 5.81 (s, 1H, NH), 3.02, 2.99 (2t, 4H, 2 CH_2), 2.20 (s, 3H, CH_3), 1.78, 1.75 (2 m, 4H, 2 CH_2). ^{13}C NMR (100 MHz, DMSO-d_6) δ 165.3 (C=O), 155.2 (*C*-CH_3), 148.3, 146.1, 144.5, 140.1, 138.5, 128.9, 128.6, 128.5, 115.9 (aromatic, C-H), 115.5 (CN), 103.1 (*C*-CN), 29.1, 28.2, 26.2, 23.3 (CH_2), 20.5 (CH_3). MS (*m/z*): M^+ 315 (25%). Anal. Calcd for $C_{20}H_{17}N_3O$ (315.14): % C, 76.17; H, 5.43; N, 13.32. Found: % C, 76.20; H, 5.39; N, 13.36.

Reaction of 1 with phenyl iso(thio)cyanate

Compound **1** (0.001 mol) in phenyl isocyanate or phenyl isothiocyanate acid (10 mL) was refluxed for 10 h then it was poured into ice-water (40 mL) to give a precipitate that recrystallized from EtOH to furnish **8a**,**b**.

1-Imino-3-oxo-2,6-diphenyl-1,2,3,4,7,8,9,10-octahydrobenzo[*f*]quinazoline-5-carbonitrile (8a): Golden yellow crystals in 65% yield: mp 124-126 ºC (EtOH). IR (KBr, cm^{-1}): 3205 (NH), 3050 (CH-Ar), 2980 (CH aliph), 2220 (CN), 1650 (C=O). ^{1}H NMR (400 MHz, DMSO-d_6) δ 7.63-7.02 (m, 11H, $CH_{arom,}$ NH), 5.91 (s, 1H, NH), 3.22, 2.89 (2t, 4H, 2 CH_2), 2.20, 1.96 (2 m, 4H, 2 CH_2). ^{13}C NMR (100 MHz, DMSO-d_6) δ 155.3 (C=O), 149.2, 143.3, 142.1, 139.1, 138.5, 132.9, 131.2, 129.4, 129.0, 128.9, 128.8, 128.6, 128.2, 127.9, 127.4, 106.2 (aromatic, C-H), 115.4 (CN), 100.1 (*C*-CN), 29.9, 28.5, 26.5, 23.7 (CH_2). MS (*m/z*): M^+ 392 (35%). Anal. Calcd for $C_{25}H_{20}N_4O$ (392.16): % C, 76.51; H, 5.14; N, 14.28. Found: % C, 76.55; H, 5.10; N, 14.33.

1-Imino-2,6-diphenyl-3-thioxo-1,2,3,4,7,8,9,10-octahydrobenzo[*f*]quinazoline-5-carbonitrile (8b): Yellow crystals in 75% yield: mp 159-161 ºC (EtOH). IR (KBr, cm^{-1}): 3195 (NH), 3048 (CH-Ar), 2979 (CH aliph), 2215 (CN), 1256 (C=S). ^{1}H NMR (400 MHz, DMSO-d_6) δ 9.01 (s, 1H, NH), 7.62-7.21 (m, 10H, CH_{arom}), 6.61 (s, 1H, NH), 3.35, 2.82 (2t, 4H, 2 CH_2), 2.06, 1.99 (2 m, 4H, 2 CH_2). ^{13}C NMR (100 MHz, DMSO-d_6) δ 175.3 (C=S), 147.2, 142.3, 140.1, 138.5, 138.1, 137.5, 133.9, 129.4, 128.5, 128.2, 127.6, 126.2, 107.2 (aromatic, C-H), 115.4 (CN), 105.1 (*C*-CN), 28.9, 28.5, 23.5 (CH_2). MS (*m/z*): M^+ 408 (35%). Anal. Calcd for $C_{25}H_{20}N_4S$ (408.14): % C, 73.50; H, 4.93; N, 13.71; S, 7.85. Found: % C, 73.53; H, 4.96; N, 13.67.

Ethyl *N*-(1,3-dicyano-4-phenyl-5,6,7,8-tetrahydronaphthalen-2-yl)formimidate (9): Triethyl orthoformate (25 mL), and acetic anhydride (1 mL) were added to compound **1** (0.01 mole), and refluxed for 10 h. Then excess ester was driven off, with addition of petroleum ether to afford crystalline compound **9**. Pale brown crystals in 55% yield: mp 145-147 ºC (EtOH). IR (KBr, cm^{-1}): 3052 (CH-Ar), 2985 (CH aliph), 2225, 2215 (CN). ^{1}H NMR (400 MHz, DMSO-d_6) δ 7.56-7.35 (m, 5H, CH_{arom}), 6.87 (s, 1H, =CH-O), 3.89 (q, 2H, CH_2), 3.14, 2.72 (2t, 4H, 2 CH_2), 1.88, 1.78 (2 m, 4H, 2 CH_2), 1.34 (t, 3H, CH_3). ^{13}C NMR (100 MHz, DMSO-d_6) δ 172.3 (=CH-O), 149.2, 147.3, 146.1, 139.1, 138.5, 133.9, 128.6, 128.2 (aromatic,

C-H), 116.1, 115.5 (2 CN), 107.1, 98.1 (2 *C*-CN), 64.3, 28.2, 28.3, 23.2 (CH_2), 13.1 (CH_3). MS (*m/z*): M^+ 329 (15%). Anal. Calcd for $C_{21}H_{19}N_3O$ (329.15): % C, 76.57; H, 5.81; N, 12.76. Found: % C, 76.60; H, 5.84; N, 12.72.

2-Amino-1-imino-6-phenyl-1,2,7,8,9,10-hexahydrobenzo[*f*]quinazoline-5-carbonitrile (10): Hydrazine hydrate (0.01 mole) was added to **9** (0.01 mole), in 30 mL of EtOH under stirring at room temperature for 5 min. then it was poured into ice-water (40 mL) to give a precipitate that recrystallized from EtOH to furnish **10**.

Pale brown crystals in 66% yield: mp 178-180 ºC (EtOH). IR (KBr, cm^{-1}): 3290 (NH_2), 2190 (NH), 3050 (CH-Ar), 2978 (CH aliph), 2215 (CN). ^{1}H NMR (400 MHz, DMSO-d_6) δ 9.28 (s, 1H, pyrimidine CH), 7.58-7.35 (m, 5H, CH_{arom}), 6.06 (s, 1H, NH), 3.23, 2.78 (2t, 4H, 2 CH_2), 2.98 (s, 1H, NH_2), 1.98, 1.96 (2 m, 4H, 2 CH_2). ^{13}C NMR (100 MHz, DMSO-d_6) δ 147.3, 142.1, 144.5, 141.2, 139.5, 138.5, 128.9, 128.6, 128.4, 128.2, 128.0, 127.5, 103.6, 110.1 (aromatic, C-H), 115.9 (CN), 29.5, 28.5, 28.2, 23.2 (CH_2). MS (*m/z*): M^+ 315 (15%). Anal. Calcd for $C_{19}H_{17}N5$ (315.15): % C, 72.36; H, 5.43; N, 22.21. Found: % C, 72.40; H, 5.39; N, 22.25.

1-Amino-3,6-diphenyl-7,8,9,10-tetrahydrobenzo[*f*]quinoline-2,5-dicarbonitrile (11): 2-Benzylidenemalononitrile (prepared *via* condensation of malononitrile and benzaldehyde) was reacted with **1** in EtOH at reflux temperature for 15 h. After reaction completion, it poured into ice-water (40 mL) to give a solid precipitate **11** as brown crystals in 62% yield: mp 278-280 ºC (EtOH). IR (KBr, cm^{-1}): 3290 (NH_2), 3050 (CH-Ar), 2978 (CH aliph), 2220 (CN). ^{1}H NMR (400 MHz, DMSO-d_6) δ 7.90-7.35 (m, 10H, CH_{arom}), 3.19, 2.76 (2t, 4H, 2 CH_2), 1.98 (s, 1H, NH_2), 1.79, 1.76 (2 m, 4H, 2 CH_2). ^{13}C NMR (100 MHz, DMSO-d_6) δ 156.2 (pyridine C-Ph), 148.3, 143.4, 141.1, 139.8, 139.5, 138.5, 136.4, 131.1, 128.5, 128.2, 122.3, 110.1 (aromatic, C-H), 119.2, 117.9 (CN) 82.3 (*C*-CN), 29.5, 29.2, 24.2, 23.2 (CH_2). MS (*m/z*): M^+ 400 (15%). Anal. Calcd for $C_{27}H_{20}N_4$ (400.17): % C, 80.98; H, 5.03; N, 13.99. Found: % C, 80.95; H, 5.07; N, 13.94.

Ethyl 1-amino-5-cyano-3-methyl-6-phenyl-7,8,9,10-tetrahydrobenzo[*f*]quinoline-2-carboxylate (12): Ethyl acetoacetate was reacted with **1** at reflux temperature for 15 h. After reaction completion, it poured into ice-water (40 mL) to give a solid precipitate **12** as yellow crystals in 60% yield: mp 255-257 ºC (EtOH). IR (KBr, cm^{-1}): 3280 (NH_2), 3050 (CH-Ar), 2978 (CH aliph), 2210 (CN). ^{1}H NMR (400 MHz, DMSO-d_6) δ 7.59-7.37 (m, 5H, CH_{arom}), 4.35 (q, 2H, CH_2), 2.85, 2.74 (2t, 4H, 2 CH_2), 1.95 (s, 1H, NH_2), 1.78, 1.38 (2 m, 4H, 2 CH_2). ^{13}C NMR (100 MHz, DMSO-d_6) δ 165.6 (C=O), 162.5 (cyclic C-NH_2), 155.2 (pyridine *C*-Me), 153.2, 143.3, 141.1, 138.8, 138.5, 128.9, 128.5, 128.2, 126.5, 122.8, 110.7 (aromatic, C-H, CN), 82.3 (*C*-CN), 61.2, 29.5, 28.2, 23.2 (CH_2), 14.2 (CH_3). MS (*m/z*): M^+ 385 (15%). Anal. Calcd for $C_{24}H_{23}N_3O_2$ (385.18): % C, 74.78; H, 6.01; N, 10.90. Found: % C, 74.81; H, 5.98; N, 10.86.

Reaction of 1 with diamine: To a mixture of compound **1** (0.002 mol) and ethylenediamine or *o*-

phenylenediamine (5 mL), carbon disulfide (1 mL) was added dropwise with stirring at room temperature. The reaction mixture was heated on water bath for 5 h. The formed precipitate was filtered off, dried and recrystallized from EtOH to give compound **13a**,**b**.

The forgoing procedures for preparation of **13a**,**b** were repeated except that ethylenediamine or *o*-phenylenediamine (10 mL) carbon disulfide (2 mL) was replaced by to give **13c**,**d**.

3-Amino-4-(4,5-dihydro-1*H*-imidazol-2-yl)-1-phenyl-5,6,7,8-tetrahydronaphthalene-2-carbonitrile (13a): Pale red crystals in 45% yield: mp 196-198 ºC (EtOH). IR (KBr, cm^{-1}): 3250 (NH_2), 3100 (NH), 3045 (CH-Ar), 2975 (CH aliph), 2220 (CN). ^{1}H NMR (400 MHz, DMSO-*d*$_6$) δ 7.55-7.35 (m, 5H, CH_{arom}), 4.35 (s, 2H, NH_2), 3.92, 3.47, 3.10, 2.94 (4t, 8H, 4 CH_2), 1.96 (s, 1H, NH), 1.76 (m, 4H, 2 CH_2). ^{13}C NMR (100 MHz, DMSO-*d*$_6$) δ 155.6 (C, imidazole), 152.5 (cyclic C-NH_2), 142.3, 141.6, 138.6, 138.4, 128.5, 128.2, 121.8, 113.7 (aromatic, C-H, CN), 57.2, 47.2, 28.5, 23.2 (CH_2). MS (*m/z*): M^+ 316 (35%). Anal. Calcd for $C_{20}H_{20}N_4$ (316.17): % C, 75.92; H, 6.37; N, 17.71. Found: % C, 75.95; H, 6.33; N, 17.75.

3-Amino-4-(1*H*-benzo[*d*]imidazol-2-yl)-1-phenyl-5,6,7,8-tetrahydronaphthalene-2-carbonitrile (13b): Red crystals in 48% yield: mp 211-213 ºC (EtOH). IR (KBr, cm^{-1}): 3255 (NH_2), 3110 (NH), 3045 (CH-Ar), 2975 (CH aliph), 2219 (CN). ^{1}H NMR (400 MHz, DMSO-*d*$_6$) δ 7.64-7.24 (m, 10H, CH_{arom}, NH), 5.35 (s, 2H, NH_2), 3.15, 2.94 (2t, 4H, 2 CH_2), 1.78 (m, 4H, 2 CH_2). ^{13}C NMR (100 MHz, DMSO-*d*$_6$) δ 157.6 (cyclic C-NH_2), 144.3, 137.6, 135.4, 132.5, 128.5, 128.2, 118.7, 115.2, 102.6 (aromatic, C-H, CN), 28.5, 23.2 (CH_2). MS (*m/z*): M^+ 364 (35%). Anal. Calcd for $C_{24}H_{20}N_4$ (364.17): % C, 79.10; H, 5.53; N, 15.37. Found: % C, 79.14; H, 5.50; N, 15.40.

1,3-Bis(4,5-dihydro-1*H*-imidazol-2-yl)-4-phenyl-5,6,7,8-tetrahydronaphthalen-2-amine (13c): Pale red crystals in 35% yield: mp 156-158 ºC (EtOH). IR (KBr, cm^{-1}): 3260 (NH_2), 3110 (NH), 3048 (CH-Ar), 2980 (CH aliph). ^{1}H NMR (400 MHz, DMSO-*d*$_6$) δ 7.56-7.34 (m, 5H, CH_{arom}), 4.30 (s, 2H, NH_2), 3.98, 3.86, 3.77, 3.47, 2.98, 2.51 (6t, 2H, 6 CH_2), 2.01, 1.66 (2 s, 2H, 2 NH), 1.76 (m, 4H, 2 CH_2). ^{13}C NMR (100 MHz, DMSO-*d*$_6$) δ 155.6, 153.2 (C, imidazole), 149.5 (cyclic C-NH_2), 144.3, 138.5, 137.0, 133.1, 128.8, 128.7, 115.9, 113.8 (aromatic, C-H), 57.2, 45.2, 29.5, 23.1 (CH_2). MS (*m/z*): M^+ 359 (35%). Anal. Calcd for $C_{22}H_{25}N_5$ (359.21): % C, 73.51; H, 7.01; N, 19.48. Found: % C, 73.48; H, 7.05; N, 19.44.

1,3-Bis(1*H*-benzo[*d*]imidazol-2-yl)-4-phenyl-5,6,7,8-tetrahydronaphthalen-2-amine (13d): Red crystals in 36% yield: mp 175-177 ºC (EtOH). IR (KBr, cm^{-1}): 3265 (NH_2), 3120 (NH), 3055 (CH-Ar), 2985 (CH aliph). ^{1}H NMR (400 MHz, DMSO-*d*$_6$) δ 7.59-7.20 (m, 15H, CH_{arom}, NH), 4.85 (s, 2H, NH_2), 3.27, 2.61 (2t, 4H, 2 CH_2), 1.77 (m, 4H, 2 CH_2). ^{13}C NMR (100 MHz, DMSO-*d*$_6$) δ 152.6 (cyclic C-NH_2), 138.6, 137.5, 135.4, 133.5, 132.5, 128.5, 123.2, 118.7, 115.2, 112.6 (aromatic, C-H), 28.5, 23.2 (CH_2). MS (*m/z*): M^+ 455 (35%). Anal. Calcd for $C_{30}H_{25}N_5$ (455.21): % C, 79.10; H, 5.53; N, 15.37. Found: % C, 79.15; H, 5.50; N, 15.40.

MATERIALS AND METHOD OF ANTITUMOR SCREENING

IN VITRO CYTOTOXIC ACTIVITY

SUPPORTING INFORMATION

Supplementary (synthesis of the starting azides, HPLC chromatograms, IR, 1H and 13C NMR, MS spectra, etc.) data associated with this article can be found, in the online version, at URL: https://www.heterocycles.jp/newlibrary/downloads/PDFsi/27697/104/11

MTT CYTOTOXICITY ASSAY

The cytotoxicity activity against HepG2 and MCF-7 human cancer cell lines[19] (*See supporting information*)

METHODS:

SYSTEM PREPARATION

The X-ray crystal structures of DNA dodecamer (CGCAAATTTGCG) with a bifurcated hydrogen-bonded conformation of the AT base pairs and its complex. Distamycin was retrieved from the protein data bank with codes 2DND.[20] These structures were then prepared for molecular dynamics (MD) studies using UCSF Chimera.[21] Using PROPKA, pH was fixed and optimized to 7.5.[22] Compounds **3b** and **6** were drawn using ChemBioDraw Ultra 12.1.[23] Altogether, all two prepared systems were subjected to 50 ns MD simulations as described in the simulation section.

MOLECULAR DYNAMICS (MD) SIMULATIONS

The integration of molecular dynamics (MD) simulations in biological systems' study enable exploring the physical motion of atoms and molecules that cannot be easily accessed by any other means.[24] The insight extracted from performing this simulation provides an intricate perspective into the biological systems' dynamical evolution, such as conformational changes and molecule association.[24] The MD simulations of all systems were performed using the GPU version of the PMEMD engine present in the AMBER 18 package.[25]

The partial atomic charge of each compound was calculated with ANTECHAMBER's General Amber Force Field (GAFF) technique.[26] The Leap module of the AMBER 18 package implicitly solvated each system within an orthorhombic box of TIP3P water molecules within 10 Å of any box edge. The Leap module was used to neutralize each system by incorporating Na^+ and Cl^- counter ions. A 2000-step initial minimization of each system was carried out in the presence of a 500 kcal/mol applied restraint potential, followed by a 1000-step full minimization using the conjugate gradient algorithm without restraints.

During the MD simulation, each system was gradually heated from 0 K to 300 K over 500 ps, ensuring that

all systems had the same amount of atoms and volume. The system's solutes were subjected to a 10 kcal/mol potential harmonic constraint and a 1 ps collision frequency. Following that, each system was heated and equilibrated for 500 ps at a constant temperature of 300 K. To simulate an isobaric-isothermal (NPT) ensemble, the number of atoms and pressure within each system for each production simulation were kept constant, with the system's pressure maintained at 1 bar using the Berendsen barostat.[27]

For 50 ns, each system was MD simulated. The SHAKE method was used to constrain the hydrogen bond atoms in each simulation. Each simulation used a 2 fs step size and integrated an SPFP precision model. An isobaric-isothermal ensemble (NPT) with randomised seeding, constant pressure of 1 bar, a pressure-coupling constant of 2 ps, a temperature of 300 K, and a Langevin thermostat with a collision frequency of 1 ps was used in the simulations.

POST-MD ANALYSIS

After saving the trajectories obtained by MD simulations every 1 ps, the trajectories were analyzed using the AMBER18 suite's CPPTRAJ[28] module. The Origin[29] data analysis program and Chimera[21] were used to create all graphs and visualizations.

THERMODYNAMIC CALCULATION

The Poisson-Boltzmann or generalized Born and surface area continuum solvation (MM/PBSA and MM/GBSA) approach has been found to be useful in the investigation of a wide range of nucleic acid systems.[30] The DNA-Ligand complex molecular simulations used by MM/GBSA and MM/PBSA compute rigorous statistical-mechanical binding free energy within a defined force field.[31]

Binding free energy averaged over 500 snapshots extracted from the entire 50 ns trajectory. The estimation of the change in binding free energy (ΔG) for each molecular species (complex, ligand, and receptor) can be represented as follows:[32]

$$\Delta G_{bind} = G_{complex} - G_{receptor} - G_{ligand} \quad (1)$$

$$\Delta G_{bind} = E_{gas} + G_{sol} - TS \quad (2)$$

$$E_{gas} = E_{int} + E_{vdw} + E_{ele} \quad (3)$$

$$G_{sol} = G_{GB} + G_{SA} \quad (4)$$

$$G_{SA} = \gamma SASA \quad (5)$$

The terms Egas, Eint, Eele, and Evdw symbolize the gas-phase energy, internal energy, Coulomb energy, and van der Waals energy. The E_{gas} was directly assessed from the FF14SB force field terms. Solvation-free energy (G_{sol}) was evaluated from the energy involvement from the polar states (G_{GB}) and non-polar

states (G). The non-polar solvation free energy (G_{SA}) was determined from the Solvent Accessible Surface Area (SASA)[33] using a water probe radius of 1.4 Å. In contrast, solving the GB equation assessed the polar solvation (GGB) contribution. Items S and T symbolize the total entropy of the solute and temperature, respectively.

ACKNOWLEDGMENT

The authors thank the National Research Centre for the financial support. Also, they thank Biochemistry department, Faculty of Pharmacy, Ain-Shams University for antitumor screening.

CONFLICT OF INTEREST

The authors have no conflict of interest.

REFERENCES

1. T. P. Selvam and P. V. Kumar, *Research in Pharmacy*, 2011, **11**, Corpus ID 101872419.
2. (a) H. B. Borate, A. S. Kudale, and S. G. Agalave, *Org. Prep. Proced. Int.*, 2012, **44**, 467; (b) A. M. Shestopalov, A. A. Shestopalov, and L. A. Rodinovskaya, *Synthesis*, 2008, 1.
3. (a) M. N. Elinson, A. I. Ilovaisky, V. M. Merkulova, F. Barba, and B. Batanero, *Tetrahedron*, 2013, **69**, 7125; (b) V. P. R. Gajulapalli, P. Vinayagam, and V. Kesavan, *RSC Adv.*, 2015, **5**, 7370; (c) I. R. Siddiqui, S. Shamim, M. A. Waseem, A. Srivastava, and Rahila, *RSC Adv.*, 2013, **3**, 14423; (d) R. R. Kumar, S. Perumal, J. C. Menéndez, P. Yogeeswari, and D. Sriram, *Bioorg. Med. Chem.*, 2011, **19**, 3444.
4. M. G. Barthakur, A. Hasib, J. Gogoi, and R. C. Boruah, *Steroids*, 2010, **75**, 445.
5. M. Hammouda, A. El-Ahl, Y. El-Toukhee, and M. Metwally, *J. Chem. Res.*, 2002, **2002**, 89.
6. A. Khodairy, A. El-Sayed, H. Salah, and H. Abdel-Ghany, *Synth. Commun.*, 2007, **37**, 3245.
7. (a) A. Herrera, R. Martínez-Alvarez, M. Chioua, R. Chatt, R. Chioua, A. Sánchez, and J. Almy, *Tetrahedron*, 2006, **62**, 2799; (b) L. Yang and R. Hua, *Chem. Lett.*, 2013, **42**, 769.
8. (a) A. E. Sutton, T. E. Richardson, B. R. Huck, S. R. Karra, X. Chen, Y. Xiao, A. Goutopoulos, R. Lan, D. Perrey, and H. G. Vandeveer, Amino azaheterocyclic carboxamides. Google Patents: USA8637532B2, 2015; (b) A. E. G. Hammam, N. A. A. El-hafeza, W. H. Midurab, and M. Mikołajczyk, *Z. Naturforsch. B*, 2000, **55**, 417; (c) M. S. A. E.-A. El-Gaby, S. G. Abdel-Hamide, M. M. Ghorab, and S. M. El-Sayed, *Acta Pharm.*, 1999, **49**, 149.
9. (a) A. El-Wahab, A. Bedair, F. Eid, A. El-Haddad, A. A. El-Deeb, and G. El-Sherbiny, *J. Serbian Chem. Soc.*, 2006, **71**, 471; (b) A. Chowdhury, M. Matin, and M. Anwar, *Chittagong University Studies, Part II: Science*, 1997, **21**, 79.

10. M. N. Nasr and M. M. Gineinah, *Arch. Pharm.*, 2002, **335**, 289.
11. G. Mangalagiu, M. Ungureanu, G. Grosu, I. Mangalagiu, and M. Petrovanu, *Ann. Pharm. Fr.*, 2001, 139.
12. (a) C. Balakumar, P. Lamba, D. P. Kishore, B. L. Narayana, K. V. Rao, K. Rajwinder, A. R. Rao, B. Shireesha, and B. Narsaiah, *Eur. J. Med. Chem.*, 2010, **45**, 4904; (b) S. M. Sondhi, M. Johar, S. Rajvanshi, S. G. Dastidar, R. Shukla, R. Raghubir, and J. W. Lown, *Aust. J. Chem.*, 2001, **54**, 69.
13. (a) N. M. Ibrahim, H. A. Yosef, E. F. Ewies, M. R. Mahran, M. M. Ali, and A. E. Mahmoud, *J. Braz. Chem. Soc.*, 2015, **26**, 1086; (b) R. S. Gouhar, E. F. Ewies, M. F. El-Shehry, M. N. Shaheen, and E. M. M. Ibrahim, *J. Heterocycl. Chem.*, 2018, **55**, 2368.
14. (a) T. Indumathi, F. R. Fronczek, and K. R. Prasad, *Synth. Commun.*, 2014, **44**, 1760; (b) M. M. Mojtahedi, L. Pourabdi, M. S. Abaee, H. Jami, M. Dini, and M. R. Halvagar, *Tetrahedron*, 2016, **72**, 1699; (c) H. M. Faidallah, K. M. A. Al-Shaikh, T. R. Sobahi, K. A. Khan, and A. M. Asiri, *Molecules*, 2013, **18**, 15704.
15. X. Liu, S. Ouyang, B. Yu, Y. Liu, K. Huang, J. Gong, S. Zheng, Z. Li, H. Li, and H. Jiang, *Nucleic Acids Res.*, 2010, **38**, W609.
16. (a) S.-Y. Chiang, J. Welch, F. J. Rauscher III, and T. A. Beerman, *Biochem. Cell Biol.*, 1994, **33**, 7033; (b) J. J. Welchi, F. Rauscher, and T. Beermani, *J. Biol. Chem*, 1994, **269**, 31051.
17. K. E. Machaba, N. N. Mhlongo, and M. E. Soliman, *Cell Biochem. Biophys.*, 2018, **76**, 345.
18. Z. Cournia, B. Allen, and W. Sherman, *J. Chem. Inf. Model.*, 2017, **57**, 2911.
19. (a) J. Van Meerloo, G. J. Kaspers, and J. Cloos, In *Cancer Cell Culture*, Springer, 2011, 237; (b) E. F. Ewies, M. El-Hussieny, N. F. El-Sayed, M. M. Ali, and A. E. Mahmoud, *Phosphorus, Sulfur Silicon Relat. Elem.*, 2016, **191**, 1000; (c) N. F. El-Sayed, E. F. Ewies, M. El-Hussieny, L. S. Boulos, and E. M. Shalaby, *Z. Naturforsch. B*, 2016, **71**, 765.
20. M. Coll, C. A. Frederick, A. Wang, and A. Rich, *Proc. Natl. Acad. Sci. USA*, 1987, **84**, 8385.
21. E. F. Pettersen, T. D. Goddard, C. C. Huang, G. S. Couch, D. M. Greenblatt, E. C. Meng, and T. E. Ferrin, *J. Comput. Chem.*, 2004, **25**, 1605.
22. H. Li, A. D. Robertson, and J. H. Jensen, *Proteins*, 2005, **61**, 704
23. R. Halford, *Chem. Eng. News*, 2014, **92**, 26.
24. A. Hospital, J. R. Goñi, M. Orozco, and J. L. Gelpí, *Adv. Appl. Bioinform. Chem.*, 2015, **8**, 37.
25. T.-S. Lee, D. S. Cerutti, D. Mermelstein, C. Lin, S. LeGrand, T. J. Giese, A. Roitberg, D. A. Case, R. C. Walker, and D. M. York, *J. Chem. Inform.*, 2018, **58**, 2043.
26. J. Wang, W. Wang, P. A. Kollman, and D. A. Case, *J. Mol Graph. Model.*, 2006, **25**, 247.
27. H. J. Berendsen, J. V. Postma, W. F. van Gunsteren, A. DiNola, and J. Haak, *J. Chem. Phys.*, 1984, **81**, 3684.

28. D. R. Roe and T. E. Cheatham III, *J. Chem. Theory Compt.*, 2013, **9**, 3084.
29. E. Seifert, OriginPro 9.1: Scientific Data Analysis and Graphing Software Software Review. *ACS Publication*, 2014.
30. (a) J. Srinivasan, T. E. Cheatham, P. Cieplak, P. A. Kollman, and D. A. Case, *J. Am. Chem. Soc.*, 1998, **120**, 9401; (b) P. A. Kollman, I. Massova, C. Reyes, B. Kuhn, S. Huo, L. Chong, M. Lee, T. Lee, Y. Duan, W. Wang, O. Donini, P. Cieplak, J. Sirinivasan, D. A. Case, and T. E. Cheatham, *Acc. Chem. Res.*, 2000, **33**, 889; (c) J. Srinivasan, J. Miller, P. A. Kollman, and D. A. Case, *J. Biomol. Struct. Dyn.*, 1998, **16**, 671; (d) T. E. Cheatham III, J. Srinivasan, D. A. Case, and P. A. Kollman, *J. Biomol. Struct. Dyn.*, 1998, **16**, 265.
31. (a) M. Drissi, N. Benhalima, Y. Megrouss, R. Rachida, A. Chouaih, and F. Hamzaoui, *Molecules*, 2015, **20**, 4042; (b) J. M. Hayes and G. Archontis, MM-GB (PB) SA calculations of protein-ligand binding free energies. In *Molecular Dynamics-Studies of Synthetic and Biological Macromolecules*, IntechOpen: 2012.
32. T. Hou, J. Wang, Y. Li, and W. Wang, *J. Chem. Inform. Model.*, 2010, **51**, 69.
33. D. Sitkoff, K. A. Sharp, and B. Honig, *J. Phys. Chem.*, 1994, **98**, 1978.